



## Recombinant Protein rP21 from *Trypanosoma cruzi* has Effect on Inflammation, Angiogenesis and Fibrogenesis in Skin Wound Model C57BL/6 Mouse

Jeranice Silva Barbosa<sup>1</sup>, Francielle Borges Rosa de Moura<sup>1,2</sup>,  
Bruno Antonio Ferreira<sup>1,3</sup>, Flávia Alves Martins<sup>1</sup>, Elusca Helena Muniz<sup>1</sup>,  
José Augusto Leoncio Gomide<sup>3</sup>, Cláudio Vieira da Silva<sup>1</sup>,  
Daniele Lisboa Ribeiro<sup>1</sup>, Fernanda de Assis Araújo<sup>1</sup>  
and Tatiana Carla Tomiosso<sup>1\*</sup>

<sup>1</sup>Institute of Biomedical Sciences, Federal University of Uberlândia, Uberlândia, MG, Brazil.

<sup>2</sup>Institute of Biology, State University of Campinas, Campinas, SP, Brazil.

<sup>3</sup>Institute of Biotechnology, Federal University of Uberlândia, Uberlândia, MG, Brazil.

### Authors' contributions

This work was carried out in collaboration between all authors. Authors JSB, FBRM, BAF, FAM, EHM, And JALG lead the experimental model, from protein choice, treatment to biochemical and morphological tests. Authors CVS, DLR, FAA and TCT prepared and coordinated the study. All authors contributed to the writing and corrections, in addition to approving the final manuscript.

### Article Information

DOI: 10.9734/AIR/2021/v22i130285

#### Editor(s):

(1) Dr. Carmen Lizette del Toro Sánchez, University of Sonora, Mexico.

#### Reviewers:

(1) Jaqueline Mena Huertas, Universidad de Nariño, Colombia.

(2) Gretchen Flores Sandí, University of Costa Rica, Costa Rica.

Complete Peer review History: <http://www.sdiarticle4.com/review-history/65805>

Original Research Article

Received 15 December 2020

Accepted 22 February 2021

Published 13 March 2021

### ABSTRACT

**Aims:** Recombinant proteins rP2 has demonstrated biological activity in inflammation by acting on the recruitment of leukocytes and by inducing phagocytosis, also modulating the processes of angiogenesis and fibrogenesis in different experimental models. In this study we evaluated the effects of the recombinant protein rP21 from *Trypanosoma cruzi* in cutaneous wounds.

**Study Design:** The wounds were induced on the back of mice and treated with rP21 at 1 µg/mL and 50 µg/mL concentration, for 3 and 7 days.

**Study Location and Duration:** Institute of Biomedical Sciences and Animal Breeding Network and

\*Corresponding author: E-mail: [tatianatomiosso@gmail.com](mailto:tatianatomiosso@gmail.com);

Rodents of the Federal University of Uberlândia, between February 2015 and February 2016.

**Methodology:** The contraction time of wound, inflammatory cell activities (neutrophils and macrophages), angiogenesis and local collagen density were evaluated.

**Sample:** Wound induction was performed on 64 male BALB / c mice approximately 9 weeks old.

**Results:** Wounds treated with rP21 showed less closure time, in addition to exhibiting greater neutrophil activity in the initial phasis, which was reduced simultaneously with the increased macrophage activity. The rP21 also performed pro-angiogenic and pro-fibrogenic activity in this study model.

**Conclusion:** These results demonstrate for the first time the biological potential of rP21 in accelerating skin tissue repair.

*Keywords: Angiogenesis; healing; inflammation; recombinant protein; skin.*

## 1. INTRODUCTION

Wound healing develops cellular and molecular events, which aims to reestablish the organ's homeostasis. Deregulation of these mechanisms cause irregularities in the repair process, leading to wounds becoming chronic lesions [1]. The chronicity of wounds can be associated with different factors such as vascular changes, diabetes, aging or the persistence of an inflammatory state, which prolongs the healing time [1]. Additionally, chronic wounds represent a public health problem, causing physical and mental suffering to patients [2] with the estimated cost for the medical system being around US \$ 25 billion per year, affecting 6.5 million of patients [3].

Research on potential drugs exhibiting healing properties has been developed and enabled the generation of new formulations [4]. Among the new therapies proposed, the use of recombinant proteins such as the rP21 protein stands out. rP21 is a protein from *Trypanosoma cruzi* whose function is associated with cell invasion in the host organism and in parasitic replication [5]. For the performance of these activities, the parasite uses several mechanisms and promotes the modulation of inflammation, angiogenesis and fibrogenesis [5], processes that are also essential for the repair of wounds.

In a subcutaneous implant model of polyester-polyurethane sponges, the treatment with the rP21 protein interfered with the generation of fibrovascular tissue and had an inducing effect on the activity of macrophages and neutrophils [6]. Considering the importance of these events in wound healing and the ability of rP21 to act on these parameters, we seek to explore in this study the effects of topical treatment with recombinant protein P21 (rP21) on the healing of excisional wounds in a murine model.

## 2. MATERIALS AND METHODS

### 2.1 Purification of rP21

The rP21 protein was obtained by affinity chromatography technique, using a nickel column and dialysis with phosphate-saline buffer (PBS) [7]. After isolating the protein, it was quantified using Bradford [8] and run on 12% polyacrylamide gel to confirm its presence and purification status.

### 2.2 Animals

Forty-eight male BALB/c mice obtained from the rodent animal breeding network of the Federal University of Uberlândia (UFU) were used. These were 9 weeks old and weighed approximately 27 g. Animals were kept in cabinets with temperature control, 12 hours of light and 12 hours of dark, with water and *ad libitum* food.

### 2.3 Wound Induction and Treatment

The animals were anesthetized intraperitoneally with 10 mg/kg of xylazine and 100 mg/kg of ketamine (both Syntec). The dorsal region of the animals was trichotomized and then four circular wounds were induced with a 5 mm punch. The wounds were treated immediately after induction and subsequent treatments were repeated daily. The rP21 was used in treatments at concentrations of 1 µg and 50 µg, added in carbopol gel. Control group was consisted of wounds treated only with the vehicle (carbopol). These three groups, control and rP21 at concentrations of 1 µg and 50 µg were evaluated after 3 and 7 days of treatment. Each wound received 250 µl of carbopol, totaling a volume of 1 ml of treatment for the 4 wounds of the animal.

## 2.4 Wound Closure Evaluation

The wounds were photographed (Sony Cybershot 14,1 DSC W320) and had their largest and smallest diameters daily measured by a digital caliper (150 mm-Matrix). Then, the area was obtained from the following formula [9]:

$$\text{PI value: } 3.14 \times (\text{Smaller diameter} / 2) \times (\text{Large diameter} / 2)$$

After obtaining the area, the closing percentage was calculated using the following formula:

$$\text{Area measurement (\%)} = \frac{\text{area of the wound on the day treatment} - (\text{area of the wound on day 0})}{\text{area of the wound on day 0}} \times 100$$

## 2.5 Morphological Evaluation

One wound from each animal was fixed for 3 hours in metacar (Methanol: Chloroform: Acetic acid, 7:2:1). Then, the samples were embedded in paraffin and 5  $\mu\text{m}$  sectioned using the rotative microtome (MICROM / HM-315). Histological sections were stained with Toluidine Blue 0.25% for quantification of mast cells, Picrosirius Red for evaluation of types I and III collagen and Gomori's Trichomic for the quantification of blood vessels. For the quantification of mast cells and blood vessels, histological areas were obtained by photomicroscope (Leica, DM500) coupled with an image acquisition system. 10 random areas were obtained using the 400X magnification (40X objective) per animal, 8 animals per group. The quantification of collagen types I and III was performed after obtaining 10 areas of the wound region using a 20X objective, photographed with the Nikon eclipse Ti microscope, optic camera and polarization filter. The Image J program was used to quantify the parameters in the obtained images [10].

## 2.6 Hemoglobin Content Quantification

The measurement of hemoglobin in the wound samples was performed using the Drabkin method [11]. Half a wound of each animal was homogenized in 2.0mL of a hemoglobin-specific chromogenic reagent (Drabkin's reagent-Hemoglobin Labtest kit). Thus, 500  $\mu\text{L}$  of the samples were centrifuged for 40 minutes, at 10.000 x g, 4°C and filtered through 0.22  $\mu\text{m}$  filters (Millipore). The hemoglobin concentrations were calculated after reading in a spectrophotometer with a wavelength of 540 nm

(E max, Molecular devices, Sunnyvale, CA, USA) using a known standard curve (Lab-test). The results were expressed as hemoglobin concentration (micrograms) per milligram of wet weight.

## 2.7 Myeloperoxidase (MPO) Activity

Neutrophils activity can be detected using the enzyme MPO as a quantitative marker [11,12]. One wound was homogenized in 2.0mL of sodium phosphate buffer, 80 mM at pH = 6 for 15 seconds. 300 $\mu\text{L}$  of the sample were added to 600 $\mu\text{L}$  of HTAB (Hexadecyltrimethylammonium bromide - Sigma) (0.75% w/v diluted in phosphate buffer pH 6 was added). The samples were sonicated and then centrifugated at 5.000 rpm, for 10 minutes at 4°C. The supernatant (200  $\mu\text{L}$ ) was used in the enzymatic assay with 100 $\mu\text{L}$  of 0.003% hydrogen peroxide; 100  $\mu\text{L}$  of TMB (3,3, 5,5- tetramethylbenzidine - Sigma) at 6.4 mM diluted in DMSO (dimethyl sulfoxide - Merck) placed at the same time for 1 minute. The reaction was completed with the addition of 100 $\mu\text{L}$  of 4M H<sub>2</sub>SO<sub>4</sub> (sulfuric acid - Merck). The results were expressed in MPO index (Absorbance in D.O./g wet sample weight) after reading at 450 nm (E max, Molecular devices, Sunnyvale, CA, USA).

## 2.8 N- Acetyl- $\beta$ - D- Glycosaminidase (NAG) Activity

NAG activity was evaluated using the Bailey technique [11,13] which is based on the hydrolysis of p-nitrophenyl N-acetyl- $\beta$ -D-glucosamine (substrate) by N-acetyl- $\beta$ -D-glycosaminidase, releasing p-nitrophenol. NAG is a lysosomal enzyme produced by activated macrophages. Half a wound of each animal was homogenized in 2.0mL of 0.9% saline with 0.1% Triton X-100 (Promega). The homogenate was centrifuged at 3.000 rpm for 10 minutes at 4°C, the supernatant (150  $\mu\text{L}$ ) was added to 150  $\mu\text{L}$  of citrate/phosphate buffer. From this solution, 100  $\mu\text{L}$  were incubated to 100  $\mu\text{L}$  of the substrate (p-nitrophenyl-n-acetyl- $\beta$ -D-glycosaminidase-Sigma) diluted in citrate/ phosphate buffer, pH 4.5, at 37°C for 30 minutes. 0.2M glycine buffer (100  $\mu\text{L}$ ), pH 10.6 was added to the samples and standard curve and the reading was performed at a wavelength of 400nm (E max, Molecular devices, Sunnyvale, CA, USA). NAG activity was calculated from a standard p-nitrophenol curve. The results were expressed in nmol.mL<sup>-1</sup> / mg of wet weight of the sample.

## 2.9 Quantification of Soluble Collagen

The total soluble collagen in the samples was evaluated by a colorimetric assay, using the Picrosirius Red reaction [14]. Half of a wound was homogenized with 0.1% Triton X-100 PBS (30 seconds) and centrifuged at 6000g, for 10 minutes at - 4°C. The supernatant (50µL) was incubated with Picrosirius Red (50µL) for 30 minutes at 25°C. The complex formed was separated by centrifugation at 10,000g, at 10 and - 4°C. Then the supernatant was discarded and the pellet washed with 500 µL of ethanol. 1 ml of alkaline reagent (0.5 M NaOH) was added to the pellet. The absorbance was quantified at 540 nm in a microplate reader (E max, Molecular devices, Sunnyvale, CA, USA). The results were compared based on a standard collagen curve and the results expressed in µg of collagen per mg of sample.

## 2.10 Statistical Analysis

The results are generated in mean and standard error. For all tests performed, the sample n was 8 animals per group (n = 8). All numerical data were tested for normal distribution using the Kolmogorov-Smirnov test. Differences between groups were assessed with the One Way-ANOVA (InStat GraphPad® Software) for the comparison of means of normally distributed parameters followed by Bonferroni post-test, comparing treated groups with the control. The results of the were statistically different when  $p < 0.05$ . The Prism 5® program was used to perform statistics and plot the graphs.

## 3. RESULTS

### 3.1 rP21 Reduces Wound Closure Time

Confirmation of purification of rP21 is shown in Fig. 1A and the effect of treatments on wound closure is shown in Fig. 1B. An improvement of wound closure can be noticed after 4 days of treatment of 50 µg rP21 which was nearly 2 times higher than control. The animals treated with 1 µg rP21 also optimized the wound closure. However, at this low concentration, a longer treatment period was required for effectiveness, since the wound closure for rP21 was greater (58%) than the control group only after 6 days of treatment. After seven days of treatment, the groups treated with rP21 at concentrations of 1 µg and 50 µg showed wound closure area 36% and 38%, respectively, higher than the control group.

This efficiency of wound closure caused by rP21 can be observed also on macroscopic images shown in Fig. 1C.

(A) Polyacrylamide gel demonstrating the presence of the rP21 protein as 21 kDa band. (B) Percentage of wound closure area and (C) Photographs of skin showing the closure of wounds during the seven days of treatment in the control and the groups treated with the rP21 protein at concentrations of 1µg and 50µg groups. The bars indicate the variation of the standard error (SEM) with n=8. \*statistical difference compared with control  $p < 0.05$ , \*\*  $p < 0.01$  and \*\*\*  $p < 0.001$  evaluated by One-Way ANOVA, Bonferroni post-test.

### 3.2 rP21 Promotes the Increase of Local Mast Cells and Modulates the Activity of Inflammatory Cells (Neutrophils and Macrophages)

After 3 days of treatment with rP21 at both concentrations increased equally the number of mast cells at the wound site, being the quantity of the cells twice as high as in the control group (Fig. 2A). After a longer period of treatment, the number of mast cells remained significantly high ( $p < 0.0001$ ) in the groups treated with p21 while there was a reduction in the control group (Fig. 2A). The photomicrographs showing the increased number of mast cells after rP21 treatments are displayed in Fig. 2 D.

MPO evaluation showed that after 3 days of treatment rP21 increased neutrophil activity only at concentration of 50µg, which was 140% higher than control. In the same period, wounds treated with rP21 1µg showed a reduction in this activity (Fig. 2B). However, after 7 days, there was an increase of neutrophil activity on wound tissue of control group and both treatments decreased this activity similarly, being nearly 8 times lower than control (Fig. 2B).

NAG activity, associated with macrophage activity, there was no statistical difference between the analysed groups after 3 days of treatment. However, this activity has increased after 7 days of rP21 treatment with an increment of 72% and 126% for 1 µg and 50 µg concentrations, respectively, when compared with the control (Fig. 2 C).

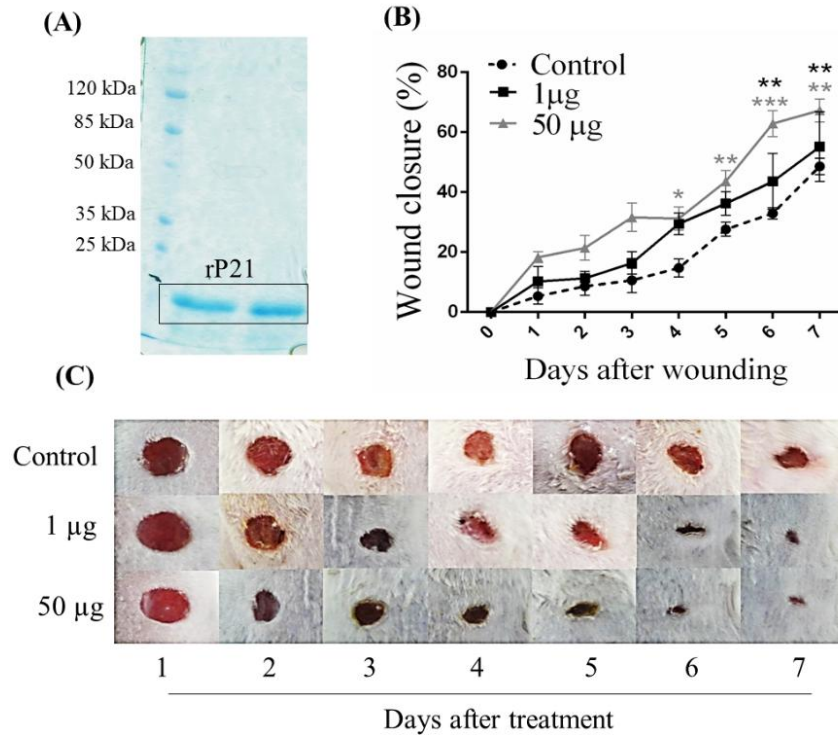


**Fig. 1. Evaluation of wound closure after treatment**

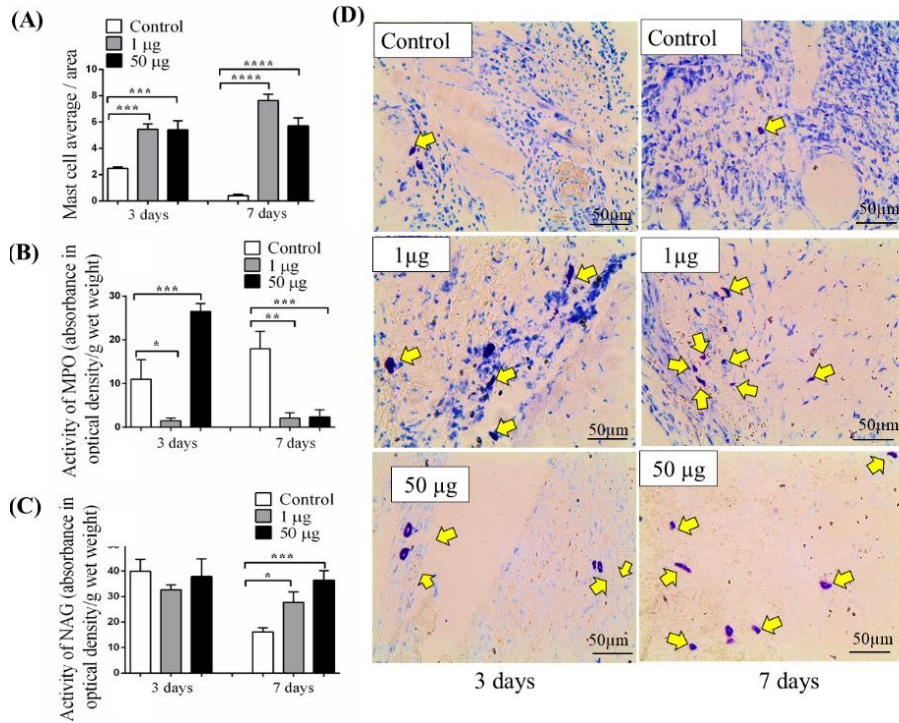


**Fig. 2. Quantification of mast cells and NAG and MPO activity in wounds**

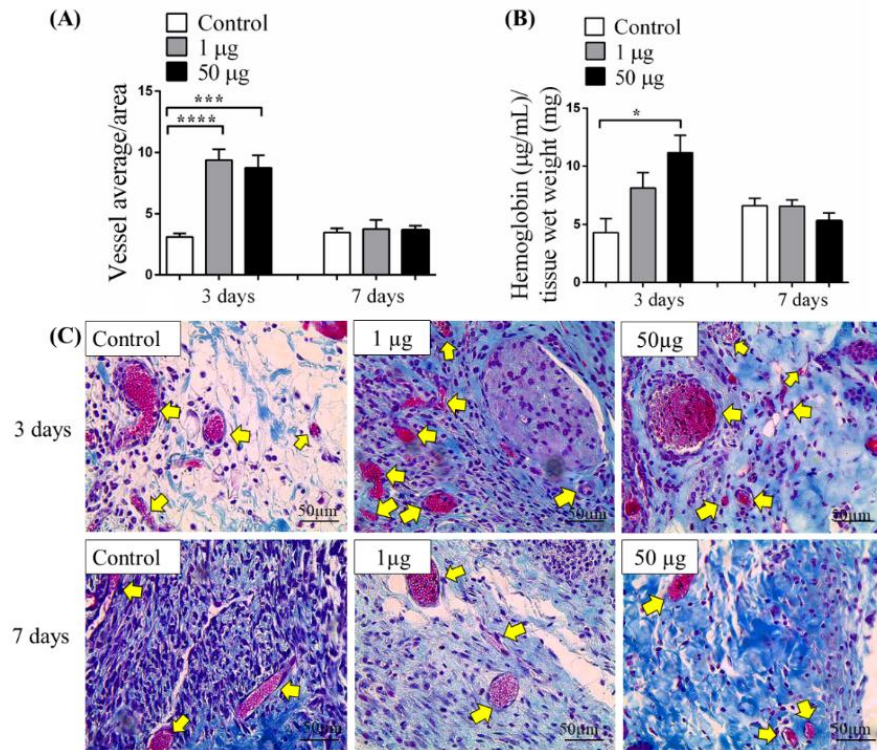


**Fig. 3. Evaluation of angiogenic activity of treatment with rP21**

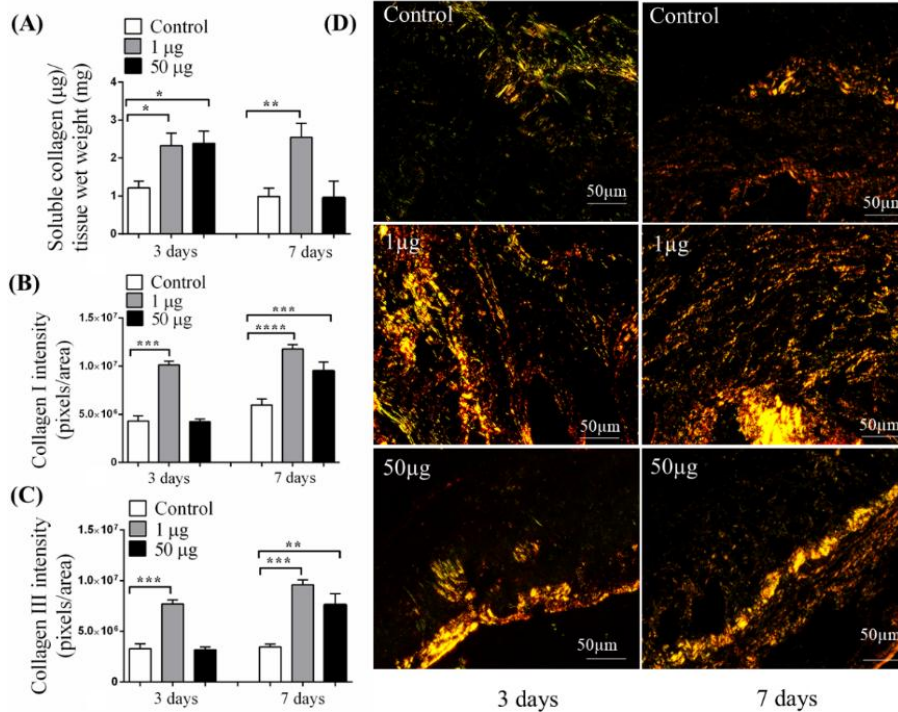


**Fig. 4. Collagen deposition in the wound area**

(A) Graphical representation of the number of mast cells (B) Myeloperoxidase enzyme activity (an indirect method to assess neutrophil activity) and (C) N-acetyl- $\beta$ -D-glycosaminidase activity (an indirect method to assess macrophage activity) in the skin wound area of rats treated as control or the rP21 protein at concentrations of 1 $\mu$ g and 50 $\mu$ g. The bars indicate the variation of the standard error (SEM) with n=8. (D) Photomicrographs of histological sections of the wound area stained with Toluidine Blue. The arrows indicate the location of mast cells. \* represents the statistical difference p<0.05, \*\* p<0.01, \*\*\* p<0.001 and \*\*\* p<0.0001 evaluated by One-Way ANOVA, Bonferroni post-test.

### 3.3 rP21 Shows Pro-angiogenic Activity in a Wound Model After 3 Days of Treatment

Fig. 3 shows the amount of blood vessels and hemoglobin in wounds after rP21 treatment. In both evaluated concentrations, 1  $\mu$ g and 50  $\mu$ g, wounds treated with rP21 showed an increase in the number of blood vessels (Fig. 3A). This increase was 202% and 182%, respectively. At longer period of 7 days, there was no difference on blood vessels content between treated groups (Fig. 3a). These data can be observed on figures of slides stained with Gomori Trichrome exhibited in Fig. 3C. Additionally, the hemoglobin content on wounds was also affected by rP21. At concentration of 50 $\mu$ g, the quantity of hemoglobins was double higher than the control's after 3 days of treatment. However, after 7 days, treatments at both concentrations did not show a different amount of hemoglobin than the control group (Fig. 3B).

Graphical representation of the number of blood vessels (A) and the measurement of hemoglobin content (B) in the skin wound area of rats treated as control or the rP21 protein at concentrations of 1 $\mu$ g and 50 $\mu$ g. The bars indicate the variation of the standard error (SEM) with n=8. (C) photomicrographs of histological wound slides stained with Gomori's Tricomoc. Blood vessels are indicated by the yellow arrows. \* represents the statistical difference considering p<0.05, \*\*\* <0.001 and \*\*\* <0.0001 evaluated by One-Way ANOVA, Bonferroni post-test.

### 3.4 rP21 Presented Pro-fibrogenic Activity in Skin Wounds

Wound treated with rP21 at both concentrations caused an increase in the soluble collagen which

was nearly 100% higher than control after 3 days of treatment. At longer period, this increase was found only in group treated with 1  $\mu$ g of rP21 (Fig. 4A). Regarding specifically type I and III, they were 135% elevated after 3 days in wounds of the 1 $\mu$ g rP21 treated group. After 7 days of treatment, type I collagen increased 97% and 50% in groups treated with 1  $\mu$ g and 50  $\mu$ g, respectively. In the same period, was noticed a higher increment of collagen III, being of 117% and 120% for the treatments of 1  $\mu$ g and 50  $\mu$ g, respectively (Fig. 4 B, C and D).

Graphical representation of the quantification of soluble collagen by the biochemical Picrosirius Red method (A); the analysis of type I (B) and Type III collagen (C) by OD- optical density in skin wounds of the control and treated with rP21 at concentrations of 1 $\mu$ g and 50 $\mu$ g. The bars indicate the variation of the standard error (SEM) with n=8. (D) Photomicrographs of slides stained with Picrosirius Red evaluated with polarization filter. Type I collagen is represented in red and type III collagen is green, the overlapping is yellow/orange. \* represents the statistical difference considering p<0.05, \*\* p<0.01, \*\*\* <0.001 and \*\*\* <0.0001 evaluated by One-Way ANOVA, Bonferroni post-test.

## 4. DISCUSSION

The treatments with rP21 protein has shown to be capable of modulating different parameters of tissue repair, leading to a consequent reduction in the time of wound closure, decreasing the risk of the exposure to infectious agents and chronification process of lesions [5]. This is the first study to evaluate the activity of rP21 and to show its effectiveness in an experimental model of wound repair.

The inflammatory response observed at the beginning of the repair process is important to eliminate invading pathogens, cellular debris and reestablish tissue dual homeostasis that initiates the subsequent stages of healing (proliferative and remodeling phases) [15]. Neutrophils are the first cells to reach the inflammatory site and, therefore, create the frontline of defense against infections since they phagocyte bacterias and eliminate part of the tissue components that were damaged during the injury [16]. 48-72 hours after the beginning of the response, the inflammatory site is predominantly populated by macrophages. Once in tissues, these cells continue the inflammatory response and orchestrate the subsequent repair [17].

Treatment with rP21 at a concentration of 50 µg was able to increase the content of macrophages near the wound area in 7 days of treatment. It has been demonstrated that rP21 is able to bind with the chemokine receptor CXCR4, with activation of the PI3-kinase pathway and consequent polymerization of the actin cytoskeleton, increasing cell migration and phagocytosis by this type of cell [18]. This activity of P21 can explain the increase of macrophages in this investigation. The ability of rP21 to increase local macrophages was also observed in a model of chronic inflammation using a subcutaneous sponge implant [6].

The reduced activity of neutrophils after the treatment with rP21 may be associated with a greater phagocytosis of these cells by macrophages recruited to the inflammatory site. In contrast, the phagocytosis of neutrophils and tissue debris is responsible for triggering phenotypical changes essential for the transition between classically activated macrophages (M1) to alternatively activated macrophages (M2) [19], a phenomenon necessary for the resolution of the inflammatory process, since M2 macrophages are the main source of anti-inflammatory mediators involved in repair [19].

Mast cells present a fundamental role in tissue repair. Mast cells are up to 8% of the dermis cell population and represent an important source of mediators, released directly into the extracellular environment or stored in its granules [20]. Treatment with rP21 during 3 or 7 days caused an increase in the number of mast cells. Such result can be due to the ability of rP21 to induce the production of cytokine IL-4. This activity of rP21 is already recognized and is closely associated with maturation, survival, proliferation and migration of mast cell [5,21] The mediators produced by mast cells are involved in a series of processes associated with the different phases of the repair process, acting from the recruitment of inflammatory cells, the promotion of angiogenesis and in the synthesis/deposition of a new extracellular matrix [20].

In addition to the effects on the inflammatory response, treatment with rP21 was able to induce the synthesis of soluble collagen and the deposition of type I and type III collagen fibers. The formation of a new extracellular matrix is an important step in the tissue repair process, providing a structural support for the

migration of new cells [22]. The increased deposition of extracellular matrix after treatment with rP21 has been demonstrated in other experimental models and is associated with the migration and proliferation of fibroblasts next to the wound area [5]. These cells also have receptors of the CXCR4 family, which rP21 has the ability to bind, indicating a possible mechanism of action [23]. In addition, the increased recruitment of fibroblasts and the activation of collagen synthesis can be explained by the cytokine profile, such as IL-4 and TGF-β1, also observed in other models, whose secretion was incited after treatment with rP21. Such cytokines are related to differentiation, migration, proliferation and collagen synthesis by fibroblasts and their conversion into myofibroblasts, assisting in wound contraction [24–27]. Concomitant with collagen synthesis, in the healing tissue there is the proliferation of endothelial cells in a process to produce new blood vessels, known as angiogenesis [28]. In this study, we observed that rP21 increased some parameters related to angiogenesis, such as hemoglobin content and the number of blood vessels, after 3 days of treatment [29]. The newly formed vessels play a critical role during the wound healing process, allowing leukocyte migration, providing the oxygen and nutrients transport into the wound and the secretion of biologically active substances [30]. Guedes-da-Silva and cols. (2015) show that during the formation of fibrovascular tissue induced by sponge implants, the intrainplantation of *T. cruzi* total antigens increased the formation of new blood vessels which was associated with the release of the VEGF [31]. Moreover, data from *in vitro* studies of murine endothelial highlight the modulatory activity of rP21 due to the direct interaction of this protein with the CXCR4 receptor, causing changes in the cytoskeleton and in the expression of profile genes associated to angiogenesis [32].

## 5. CONCLUSION

rP21 in skin wound model was able to modulate the activity of neutrophils and macrophages during the inflammatory process. In this model, rP21 had a pro-angiogenic effect and, in addition, promoted an increase in mast cells that may be involved in the pro-fibrogenic action. These factors may have a great contribution to reduce the time of wound contraction. Thus, we purpose that rP21 can be considered a promising therapy for the repair of skin wounds.



## ETHICAL APPROVAL

The experiment was approved by the Ethics Committee on the Use of Animals (CEUA, 046/17).

## ACKNOWLEDGEMENTS

We thank the Coordenação de Aperfeiçoamento de Pessoal de Nível Superior - Brasil (CAPES), Fundação de Amparo à Pesquisa do Estado de Minas Gerais FAPEMIG), Conselho Nacional de Desenvolvimento Científico e Tecnológico (CNPq) and Rede de Biotérios de Roedores (REBIR) of Federal University de Uberlândia (UFU).

## COMPETING INTERESTS

Authors have declared that no competing interests exist.

## REFERENCES

1. Cañedo-Dorantes L, Cañedo-Ayala M. Skin acute wound healing: A comprehensive review. *Int J Inflamm*; 2019.
2. Yin H, Chen CY, Liu YW, et al. *Synechococcus elongatus* PCC7942 secretes extracellular vesicles to accelerate cutaneous wound healing by promoting angiogenesis. *Theranostics* 2019;9:2678–2693.
3. Barrientos S, Brem H, Stojadinovic O, et al. Clinical application of growth factors and cytokines in wound healing. *Wound Repair Regen*. 2014;22:569–578.
4. Öhnstedt E, Lofton Tomenius H, Vågesjö E, et al. The discovery and development of topical medicines for wound healing. *Expert Opin Drug Discov*. 2019;14:485–497.  
DOI:<https://doi.org/10.1080/17460441.2019.1588879>
5. Teixeira TL, Castilhos P, Rodrigues CC, et al. Experimental evidences that P21 protein controls *Trypanosoma cruzi* replication and modulates the pathogenesis of infection. *Microb Pathog*. 2019;135:103618.  
DOI:<https://doi.org/10.1016/j.micpath.2019.103618>
6. Teixeira TL, Machado FC, Alves Da Silva A, et al. *Trypanosoma cruzi* P21: A potential novel target for chagasic cardiomyopathy therapy. *Sci Rep*. 2015;5:1–10.
7. da Silva CV, Kawashita SY, Probst CM, et al. Characterization of a 21 kDa protein from *Trypanosoma cruzi* associated with mammalian cell invasion. *Microbes Infect*. 2009;11:563–570
8. Bradford M. *Snakes of India: The Field Guide*. 1976;72:248–254.  
Available:<http://www.rotoplast.com.co/sistema-septico-domiciliario/>
9. Pinto N de CC, Cassini-Vieira P, Souza-Fagundes EM de, et al. *Pereskia aculeata* Miller leaves accelerate excisional wound healing in mice. *J Ethnopharmacol*. 2016; 194:131–136.  
DOI:<http://dx.doi.org/10.1016/j.jep.2016.09.005>
10. Rasband W. *Image J*, US. National institutes of health, Bethesda, Maryland, USA; 2011.  
Available:<http://rsb.info.nih.gov/ij>  
Available:<http://imagej.nih.gov/ij/>
11. De Moura FBR, Justino AB, Ferreira BA, et al. Pro-fibrogenic and Anti-Inflammatory potential of a polyphenol-enriched fraction from *annona crassiflora* in skin repair. *Planta Med*. 2019;85:570–577.
12. Bradley PP, Priebe DA, Christensen RD, et al. Measurement of cutaneous inflammation: Estimation of neutrophil content with an enzyme marker. *J Invest Dermatol*. 1982;78:206–209.  
DOI:<http://dx.doi.org/10.1111/1523-1747.ep12506462>
13. Bailey PJ. Sponge implants as models. *Methods Enzymol*. 1988;162:327–334.
14. Castanheira LE, Lopes DS, Gimenes SNC, et al. Angiogenic effects of BpLec, a C-type lectin isolated from *Bothrops pauloensis* snake venom. *Int J Biol Macromol*. 2017;102:153–161.  
DOI:<http://dx.doi.org/10.1016/j.ijbiomac.2017.04.012>
15. Ellis S, Lin EJ, Tartar D. Immunology of wound healing. *Curr Dermatol Rep*. 2018; 7:350–358.
16. Taylor KR, Trowbridge JM, Rudisill JA, et al. Hyaluronan fragments stimulate endothelial recognition of injury through TLR4. *J Biol Chem*. 2004;279:17079–17084.
17. Willenborg S, Lucas T, Van Loo G, et al. CCR2 recruits an inflammatory macrophage subpopulation critical for angiogenesis in tissue repair. *Blood*. 2012; 120:613–625.
18. Rodrigues AA, Clemente TM, dos Santos

- MA, et al. A recombinant protein based on trypanosoma cruzi P21 enhances phagocytosis. PLoS One. 2012;7:1–9.
19. Krzyszczyk P, Schloss R, Palmer A, et al. The role of macrophages in acute and chronic wound healing and interventions to promote pro-wound healing phenotypes. Front Physiol. 2018;9:1–22.
20. Komi DEA, Khomtchouk K, Santa Maria PL. A review of the contribution of mast cells in wound healing: Involved molecular and cellular mechanisms. Clin Rev Allergy Immunol; 2019.
21. Kalesnikoff J, Galli SJ. New developments in mast cell biology. Nat Immunol. 2008;9:1215–1223
22. Löffek S, Schilling O, Franzke CW. Series matrix metalloproteinases in lung health and disease“ edited by J. Müller-Quernheim and O”. Eickelberg number 1 in this series: Biological role of matrix metalloproteinases: A critical balance. Eur Respir J. 2011;38:191–208.
23. Griffiths K, Habel DM, Jaffar J, et al. Anti-fibrotic effects of CXCR4-targeting i-body AD-114 in Preclinical Models of Pulmonary Fibrosis. Sci Rep. 2018;8:1–15. DOI:http://dx.doi.org/10.1038/s41598-018-20811-5
24. Leask A, Abraham DJ. TGF- $\beta$  signaling and the fibrotic response. FASEB J. 2004;18:816–827
25. Margadant C, Sonnenberg A. Integrin-TGF- $\beta$  crosstalk in fibrosis, cancer and wound healing. EMBO Rep. 2010;11:97–105
26. Nguyen JK, Austin E, Huang A, et al. The IL-4/IL-13 axis in skin fibrosis and scarring: Mechanistic concepts and therapeutic targets. Arch Dermatol Res; 2019. DOI: <https://doi.org/10.1007/s00403-019-01972-3>
27. Sato T, Liu X, Basma H, et al. IL-4 induces differentiation of human embryonic stem cells into fibrogenic fibroblast-like cells. J Allergy Clin Immunol. 2011;127:1595–1603.e9. DOI:http://dx.doi.org/10.1016/j.jaci.2011.01.049.
28. Moens S, Goveia J, Stapor PC, et al. The multifaceted activity of VEGF in angiogenesis- Implications for therapy responses. Cytokine Growth Factor Rev. 2014;25:473–482. DOI:http://dx.doi.org/10.1016/j.cytogfr.2014.07.009
29. Duran CL, Howell DW, Dave JM, et al. Molecular regulation of sprouting angiogenesis. Compr Physiol. 2018;8:153–235.
30. DiPietro LA. Angiogenesis and wound repair: When enough is enough. J Leukoc Biol. 2016;100:979–984.
31. Guedes-da-Silva FH, Shrestha D, Salles BC, et al. Trypanosoma cruzi antigens induce inflammatory angiogenesis in a mouse subcutaneous sponge model. Microvasc Res. 2015;97:130–136. DOI:http://dx.doi.org/10.1016/j.mvr.2014.10.007
32. Teixeira SC, Lopes DS, Gimenes SNC, et al. Mechanistic Insights into the anti-angiogenic activity of trypanosoma cruzi protein 21 and its potential impact on the onset of chagasic cardiomyopathy. Sci Rep. 2017;7:1–14.

© 2021 Barbosa et al.; This is an Open Access article distributed under the terms of the Creative Commons Attribution License (<http://creativecommons.org/licenses/by/4.0>), which permits unrestricted use, distribution, and reproduction in any medium, provided the original work is properly cited.

Peer-review history:  
The peer review history for this paper can be accessed here:  
<http://www.sdiarticle4.com/review-history/65805>